JOURNAL OF GEOPHYSICAL RESEARCH, VOL. 98, NO. C8, PAGES 14,739–14,749, AUGUST 15, 1993

# A Mixed-Layer Study of the Formation of Levantine Intermediate Water

ALEX LASCARATOS

*Laboratory of Meteorology and Oceanography, Department of Applied Physics, University of Athens, Athens, Greece*

RICHARD G. WILLIAMS

*Center for Meteorology and Physical Oceanography, Department of Earth, Atmospheric and Planetary Sciences Massachusetts Institute of Technology, Cambridge*

ELINA TRAGOU

*Laboratory of Meteorology and Oceanography, Department of Applied Physics, University of Athens, Athens, Greece*

A mixed-layer model is used to investigate the formation of Levantine Intermediate Water (LIW) over the Eastern Mediterranean. The one-dimensional model is initialized with climatological hydrography and integrated over the Levantine basin with forcing by climatological surface fluxes. Realistic and repeated seasonal mixed-layer cycles are obtained if the annual surface heat input and water loss are offset by a parameterized horizontal advection. The model integrations show that LIW is formed during winter in the mixed layer of the Northwestern Levantine. The preferred formation region for LIW is found through idealized experiments to be controlled by the preconditioning of the hydrography, especially that of the cold, cyclonic Rhodes gyre, rather than by the pattern of the climatological fluxes. The annual-mean formation rate of LIW is estimated to be 1.0 Sv using the climatological surface fluxes. The magnitude of the annual surface fluxes alters the formation rate and modifies the formation region. An additional annual heat flux reduces the formation rate of LIW, whereas an extra cooling enhances it, as well as forming waters denser than LIW in the center of the Rhodes gyre.

## 1. INTRODUCTION

The Levantine Intermediate Water (LIW) is a particularly saline water mass in the Mediterranean that is produced in the Levantine basin. The water mass spreads at intermediate depths over the entire Mediterranean and is the major contributor to the salty and warm Mediterranean outflow into the Atlantic; in section 2, we provide a review of previous work regarding the water mass structure and the formation of LIW within the Levantine basin.

We assume that the LIW water mass is formed within the mixed layer, rather than through diabatic mixing in the stratified thermocline. We investigate this formation mechanism by integrating a mixed-layer model (described in section 3) driven by climatological surface fluxes and using climatological hydrography.

The one-dimensional model is integrated separately for each 0.5° × 0.5° grid point over the basin with a parameterized horizontal advection, which offsets the annual surface heat and water input. The mixed-layer properties then identify when and where the LIW water mass is produced (section 4). This extends the study of *Ovchinnikov and Plakhin* [1984], who examine the formation of LIW using a one-dimensional model, forced with prescribed surface temperatures and salinities, at a single location inside the Rhodes Gyre.

The mixed-layer model is used to examine how the formation of LIW is controlled by the preconditioning of the hydrography and the spatial pattern of the surface fluxes (section 5). Finally, the sensitivity of the LIW formation is examined to plausible interannual variations in the surface fluxes.



Paper number 93JC00912.
0148-0227/93/9JC-00912$05.00

## 2. REVIEW OF THE LEVANTINE BASIN

### 2.1. *General Features*

The Levantine basin is the second largest basin of the Eastern Mediterranean and is bounded by the African coast in the south, the Middle East coast in the east, and the Asia Minor coast in the north (Figure 1). The Levantine communicates to the west with the Ionian basin through the sill of the Cretan Passage, the largest water body of the Eastern Mediterranean, and with the Aegean Sea to the northwest through the eastern straits of Crete.

The Levantine basin has been the object of a number of sparse, in space and time, cruises [*Lacombe and Tchernia*, 1960; *Oren*, 1971; *Mosetti et al.*, 1972; *Ozturgut*, 1976; *Ovchinnikov*, 1965, 1966]. For many years the only available general circulation map of the Levantine was the one proposed by *Ovchinnikov* [1966] in which a large cyclonic pattern dominated the whole basin.

It is only recently though, through the international program Physical Oceanography of the Eastern Mediterranean (POEM), that large-scale coordinated surveys of the whole basin have been conducted [*UNESCO*, 1984; *Robinson et al.*, 1991; *POEM Group*, 1992]. They have revealed the existence of a number of cyclonic and anticyclonic subbasin gyres as well as the presence of an energetic mesoscale eddy field with meanders, jets, and filaments [*Hecht et al.*, 1988; *Ozsoy et al.*, 1989].

The most striking feature of the basin is the permanent,

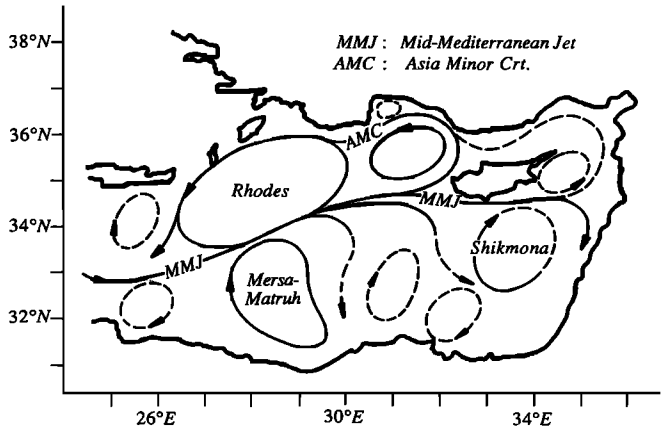


Fig. 1. A general circulation schematic showing the semipermanent gyres and currents in the Levantine basin (redrawn from *POEM Group* [1992]).

cyclonic Rhodes gyre (Figure 1), with a horizontal scale of 100 km by 200 km, situated southeast of Rhodes [*Lacombe and Tchernia*, 1960; *Ozturgut*, 1976]. It is bounded to the north by the Asia Minor Current flowing westward along the southern coast of Turkey transporting heat and salt out of the northeastern Levantine basin. The two other semipermanent gyres in the basin are the Mersa Matruh and Shikmona anticyclonic systems located north of the western Egyptian coast and south of Cyprus, respectively. In between the Rhodes gyre and these anticyclonic gyres, there is the strong meandering mid-Mediterranean jet, which is the continuation of the North African current found to the west, flowing eastward and transporting relatively fresh waters into the basin.

### 2.2. *Water Mass Structure*

The characteristic water mass structure in the Levantine basin is revealed in Figure 2 by a summer profile from *Hecht et al.* [1988], which is compiled from a series of cruises by the R/V *Shikmona* between 1979 and 1984:

1. The shallow mixed-layer contains warm and saline waters, the Levantine Surface Waters (LSW), produced by intense summer heating and evaporation. Their temperature and salinity vary within the basin and here reach typical values of 25°C and 39.1 practical salinity units (psu), respectively.

2. Below the summer mixed layer, there is a salinity minimum of typically 38.8 psu, which is not locally formed through surface forcing but results from the advection of fresher waters originating from the North Atlantic (NAW). These waters enter the Mediterranean at surface through the Gibraltar Strait with a salinity of 36.15 psu [*Lacombe and Tchernia*, 1972], and as they move eastward, their salinity increases to 37.5 at the Sicily Straits [*Morel*, 1971] and to greater than 38.6 psu in the Levantine [*Ozsoy et al.*, 1989; *Oren*, 1971]. The subsurface salinity minimum in the Levantine basin is most apparent in late summer. The disappearance of the NAW signal during winter has been attributed to both the reduced inflow of NAW through the Straits of Sicily [*Lacombe and Tchernia*, 1960; *Ovchinnikov*, 1974] and the bifurcation of the North African Current to the north off the Cyrenaica coast [*Zore-Armanda*, 1969; *Hopkins*, 1978]. However, the seasonal variation in the salinity minimum may also result from the signal of the NAW being masked by the vertical mixing in the deep winter mixed-layer (see section 4.3).

3. From 150 to 400 m, there is the Levantine Intermediate Waters (LIW), a layer of maximum salinity waters (38.95–39.05 psu) with temperatures between 15°C and 16°C. These waters are produced within the Levantine basin, then spread over the intermediate depths of both Eastern and Western Mediterranean basins (see section 2.3). They are the major contributors to the Mediterranean outflow into the Atlantic.

In Table 1, we present "core" LIW values as suggested in previous papers. We define our LIW "core" characteristics of 15°–16°C for temperature, 38.95–39.05 for salinity, and 28.85–29.10 for density; this choice then identifies when and where LIW is formed in the mixed-layer study in section 4.

4. The deep waters of Eastern Mediterranean (DW) are found at depths greater than 1500 m with temperatures of

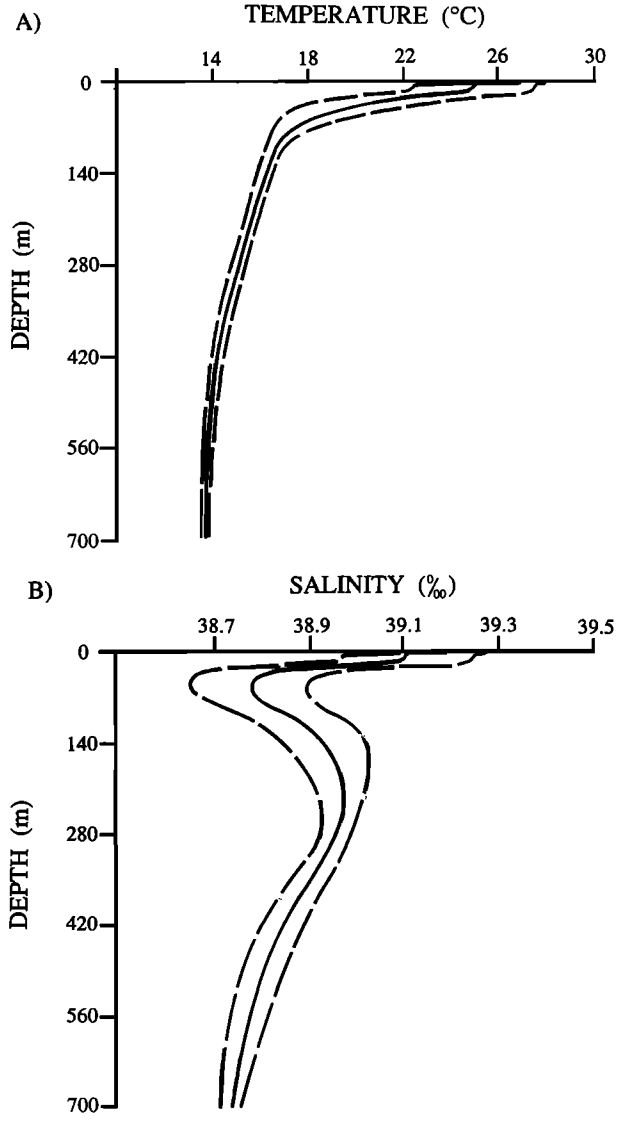


Fig. 2. Profiles of (*a*) temperature and (*b*) salinity in the Levantine basin for summer (July to October) compiled by *Hecht et al.* [1988] from R/V *Shikmona* cruises between 1979 and 1984. The solid line denotes the mean profile and the dashed lines denote one standard deviation.

TABLE 1. Water Mass Characteristics of Levantine Intermediate Water

| | Temperature, °C | Salinity, psu | $\sigma_\pm$ |
|---|---|---|---|
| *Wust* [1961] | 15.5 | 39.10 | 29.05 |
| *Lacombe and Tchernia* [1972] | 15.7 | 39.10 | 28.98 |
| *Ozturgut* [1976] | 16.2–16.4 | 39.12–39.15 | 28.85–28.87 |
| *Ovchinnikov* [1984] | 14.7–14.9 | 39.03–39.06 | 29.12–29.15 |
| *Plakhin and Smirnov* [1984] | 14.5 | 38.85 | 29.06 |
| *Hecht* [1986] | 15.5 ± 0.4 | 39.02 ± 0.05 | 28.91–29.01 |
| *Hecht et al.* [1988] | 15.5 ± 0.5 | 38.98 ± 0.06 | 28.86–28.99 |

13.6°C and salinities lower than 38.7 psu. They are believed to be produced in the Adriatic Sea [*Malanotte-Rizzoli and Hecht*, 1988; *Schlitzer et al.*, 1991]. Between the LIW and DW, there is a transition layer (TW) with intermediate characteristics [*Hecht et al.*, 1988]. These deep waters are constrained within the Eastern Mediterranean, as the sill depth is only 400 m at the Sicily Straits.

### 2.3. *Formation of Levantine Intermediate Water*

The formation region of LIW within the Levantine basin has been the object of some controversy in the past years, and at the same time, little is known about the exact mechanism of its production. *Nielsen* [1912] was the first to point toward the Rhodes gyre area as the possible source of LIW. Later, *Lacombe and Tchernia* [1960] argued that appropriate conditions for LIW formation occur in the region between Rhodes and Cyprus, while *Wust* [1961] suggested that LIW is formed in the vicinity of Rhodes both in the Levantine and the Aegean seas. *Ovchinnikov* [1984] suggests that LIW formation takes place in the Rhodes gyre area through a detailed study of the water mass characteristics of two winter cruises in the Levantine basin.

In contrast, on the basis of winter cruise data, *Ozturgut* [1976] suggests that LIW is formed within the Antalya basin and between Rhodes and the Turkish coast, since the deepest mixed layer of 300 m and the highest salinities of 39.15 are found here. On the basis of results of a 1959 winter cruise, *Morcos* [1972] suggests LIW could also be produced in the southern parts of the basin. Following the cold 1991/1992 winter, *Sur et al.* [1992] observe LIW within the mixed layer over the entire northern Levantine together with TW-DW characteristics in a deep chimney, extending to depths greater than 1 km, in the center of the Rhodes gyre.

*Ovchinnikov* [1984] has related the formation of LIW in the Rhodes gyre area to favorable dynamical and hydrodynamic conditions occurring inside this large cold, cyclonic area. Cold fluid in the center of the gyre cooled during winter significantly increase their density. The resulting water mass then sinks isopycnally to the periphery of the gyre and is arrested at intermediate depths. *Ozsoy et al.* [1989, p. 129] suggest that it should be "natural to find LIW mainly in anticyclonic eddies at the periphery of the Rhodes gyre or between the cyclonic eddies and the coast where the isopycnic sinking should be intercepted."

The layer of LIW is observed throughout all seasons at intermediate depth of typically 300 m within the thermocline of the Levantine basin. *Wust* [1961] presents evidence of a stronger outflow of LIW through the Straits of Sicily in winter, whereas *Katz* [1972] observes no such seasonal variation. *Hecht* [1986, p. 3] speculates that such constancy of flow is an indication that "LIW formation is either maintained continuously throughout the year or that it is formed in winter and released slowly and steadily during the whole year."

We believe that the band of LIW characteristics imply that it is only formed during the winter, otherwise they would have to include typical summer mixed-layer values. The nearly constant outflow of LIW through the Straits of Sicily may instead result from the annual production only accounting for a small proportion of its total volume. Indeed, according to *Ovchinnikov* [1983] the renewal time for the LIW is 25 years which means that only 4%of its total volume is renewed annually.

## 3. MIXED-LAYER MODEL

### 3.1. *Mixed-Layer Model Formulation*

A modified *Kraus and Turner* [1967] mixed-layer model is used here to investigate the seasonal cycle in the upper ocean (see *Niiler and Kraus* [1977] for a review); the model has been applied to investigate the seasonal cycle of eddies in the North Atlantic by *Williams* [1988], and similarly for a warm core eddy in the Eastern Mediterranean by *Brenner et al.* [1991].

The mixed-layer model integrates the heat and salt equations:

$$\frac{\partial T}{\partial t} + \frac{\partial}{\partial z}\overline{w'T'} = \frac{1}{\rho_0 C_w}\frac{\partial I}{\partial z} - \mathbf{u}\cdot\nabla T \tag{1}$$

$$\frac{\partial S}{\partial t} + \frac{\partial}{\partial z}\overline{w'S'} = -\mathbf{u}\cdot\nabla S \tag{2}$$

The heat and salt changes are controlled by (1) the divergence of the vertical fluxes of heat, $\overline{w'T'}$, and salt, $\overline{w'S'}$, (2) the divergence of the solar heating, $I$, for heat, and (3) the horizontal and vertical advection. The density changes are then calculated from the temperature and salt changes by using a linearized version of the equation of state:

$$\rho = \rho_0[1 - \alpha(T - T_0) + \beta(S - S_0)] \tag{3}$$

Here, $\alpha$ is the density expansion coefficient, $\beta$ is the haline contraction coefficient, $C_w$ is the heat capacity of seawater, and the subscript zero denotes reference values.

The mixed layer depth $h$ is calculated from the one-dimensional balance between the rate of production of available turbulent kinetic energy $E_\alpha$ and its rate of conversion to potential energy:

$$\frac{\partial E_\alpha}{\partial t} = g \int_{-h}^{0} \overline{w'\rho'}\, dz \tag{4}$$

Here, $g$ is gravity.

These coupled equations are solved numerically with the water column resolved into discrete depth layers. The density field is changed every hourly time step by (1) solar heating, surface heat, and water fluxes, (2) parameterized advection, (3) convective overturning, and (4) turbulent mixing; further details are given by *Woods and Barkmann* [1986] and *Williams* [1988].

### 3.2. *Mixed-Layer Model Parameterizations*

The imposed solar radiation is calculated every hour from the solar zenith angle [*List*, 1966; *Budyko*, 1974] using the monthly solar heat flux from *May* [1983]. The solar heating applied throughout the water column using an empirical profile from a three-exponential fit with constant ocean turbidity of Jerlov IA [*Horch et al.*, 1983]. The surface density flux depends on the surface heat and water fluxes:

$$\overline{w'\rho'}_{z=0} = -\alpha\rho_0\overline{w'T'}_{z=0} + \beta\rho_0\overline{w'S'}_{z=0}$$

$$= -\frac{\alpha}{C_w}(H_{ir} + H_{le} + H_{sens}) + \beta\rho_0(P - E)S_0 \tag{5}$$

Here, the surface fluxes are evaporation $E$, precipitation $P$, infrared radiation $H_{ir}$, latent heat $H_{le}$, and sensible heat $H_{sens}$; note that the solar heat flux is retained explicitly in the heat equation (1). When the mixed layer is deepening, there is entrainment of underlying denser fluid leading to a density flux at the base of the mixed layer of

$$\overline{w'\rho'}_{z=-h} = \Delta\rho \frac{dh}{dt} \tag{6}$$

where $\Delta\rho$ is the density jump at the base of the mixed layer. Naturally, there is no entrainment flux if the mixed-layer is shallowing.

### 3.3. *Parameterized Advection*

A purely one-dimensional mixed-layer model only has a closed annual cycle for special locations where there is no annual surface heat and water input. More generally, there is an annual surface input of heat and water, which is either compensated for by advection or leads to interannual variability. Assuming that there is a closed cycle and no entrainment or upwelling at the base of the seasonal thermocline, $z = -H$, then integrating the heat and salt equations over 1 year and over the seasonal boundary layer leads to

$$\int_{-H}^{0} \overline{\mathbf{u}\cdot\nabla T}\, dz = \frac{\bar{H}_{in}}{\rho_0 C_w} \tag{7}$$

$$\int_{-H}^{0} \overline{\mathbf{u}\cdot\nabla S}\, dz = \overline{(E - P)}\, S_0 \tag{8}$$

This annual balance between the surface input of heat $H_{in}$ and water $(P - E)$ with the advection of heat and salt is applied in the model in order to obtain a closed cycle [*Williams*, 1987]. Furthermore, the advection is assumed to be steady and to decay exponentially with depth:

$$\overline{\mathbf{u}\cdot\nabla T} = A_T e^{z/d} \tag{9}$$

$$\overline{\mathbf{u}\cdot\nabla S} = A_S e^{z/d} \tag{10}$$

where the coefficients $A_t = \bar{H}_{in}/[\rho_0 C_w d(1. - e^{-H/d})]$, and $A_S = \overline{(E - P)}\, S_0/[d(1. - e^{-H/d})]$, and the advection depth scale $d$ is chosen to be 35 m.

### 3.4. *Turbulent Kinetic Energy Balance*

The mixed-layer depth is calculated from the turbulent kinetic energy equation

$$\frac{\partial E_\alpha}{\partial t} = g \int_{-h}^{0} \overline{w'\rho'}\, dz$$

by comparing the rate of input of available turbulent kinetic energy $E_\alpha$ with the rate of conversion to potential energy required for entrainment (following *Thompson* [1976] and *Friedrich* [1983]).

The available turbulent mixing energy $E_\alpha$ comes from wind mixing $E_w$ and penetrative convection $E_c$, and there is some loss through dissipation $E_d$:

$$E_\alpha = E_w + E_c - E_d \tag{11}$$

The wind mixing energy depends on the imposed wind speed $u_\alpha$:

$$\frac{\partial E_w}{\partial t} = \rho_\alpha c_d m_\alpha u_\alpha^3 \tag{12}$$

Here, $c_d$ is the drag coefficient [*Large and Pond*, 1981], $m_\alpha = 1.5 \times 10^{-3}$ is the efficiency of wind mixing [*Kato and Phillips*, 1969], and $\rho_\alpha$ is the air density.

The wind mixing energy is chosen to be dissipated exponentially with depth:

$$E_d = E_w(1 - e^{-h/h_d}) \tag{13}$$

where $h$ is the previous mixed-layer depth and $h_d$ is the dissipation scale (chosen here to be 50 m).

Penetrative convection is assumed to occur whenever the surface cooling and evaporation produces a statically unstable density profile. The available turbulent kinetic energy is increased after overturning by a proportion $n = 0.12$ of the released potential energy $\Delta PE$:

$$E_c = n\Delta PE \tag{14}$$

## 4. CLIMATOLOGICAL MIXED-LAYER MODEL STUDY

### 4.1. *Climatological Surface Fluxes*

The mixed-layer model is forced using climatological heat and evaporation fluxes and wind stress data evaluated by *May* [1982, 1983]; further details on the fluxes are given by *Malanotte-Rizzoli and Bergamasco* [1991, Appendix A]). The monthly mean data over the entire Mediterranean for a 1° × 1° spatial resolution. The heat fluxes comprise solar radiation, latent heat, sensible heat, and net infrared radiation. Precipitation is taken from the *Jaeger* [1976] data set, which contains monthly data on a 5° longitudinal by 2.5° latitudinal resolution. These fluxes were interpolated linearly to a half degree spatial resolution in the Levantine basin to

match the resolution of the climatological T and S profiles used to initialize the model.

In this climatological data, there is an annual surface heat input of typically 8 W/m$^2$ over most of the Levantine basin, except for two areas in the northern region where there is a surface heat loss (Figure 3). These regions of annual heat loss appear to be controlled by the patterns of surface heat input in the summer, rather than by the surface heat loss in the winter; there are particularly high evaporative losses here in summer due to the strong northwestern winds (the Etesians) from the Aegean.

The entire Levantine basin has an annual surface water loss of typically 1.2 m/y (Figure 4) and is therefore a concentration basin. This freshwater deficit is compensated for by an excess inflow of fresher NAW through the Straits of Sicily compared with the outflow of the more saline LIW.

### 4.2. *Climatological Hydrography*

The model is initialized using temperature and salinity profiles from the climatological Generalized Digital Environmental Model (GDEM) data set for the Mediterranean Sea [*Davis et al.*, 1986; *Naval Oceanographic Office*, 1989]. The GDEM is a seasonal compilation of temperature and salinity fields, which are provided every 3 months on a half degree horizontal resolution and at the standard depths down to the seafloor. The temperature and salinity on the model levels, every 5 m, are obtained by linearly interpolating from the GDEM data.

### 4.3. *Mixed-Layer Model Profiles*

The mixed-layer model is integrated with 1-hour time steps from autumn for two different locations in the Levantine basin, first inside the Rhodes gyre at 35°N, 28°E, and second outside the gyre at 33.5°N, 28.5°E (Figure 5), using the appropriate climatological surface fluxes; at this second site, the surface fluxes and mixed-layer temperatures appear representative of the whole basin. A steady horizontal advection of heat and salt is incorporated to offset the annual surface heat input and water loss and to attain a repeated annual cycle (discussed in sections 3.3 and 4.4.2).

Over the heating season the mixed-layer shallows to a minimum depth around the summer solstice (when there is a maximum in the solar heating) with the temperature and salinity continuing to increase in late summer, until the entrainment dominates over the surface forcing. Over the cooling season, the mixed-layer continues to deepen, cool, and freshen until it reaches its maximum depth and minimum temperature and salinities at the end of winter in March.

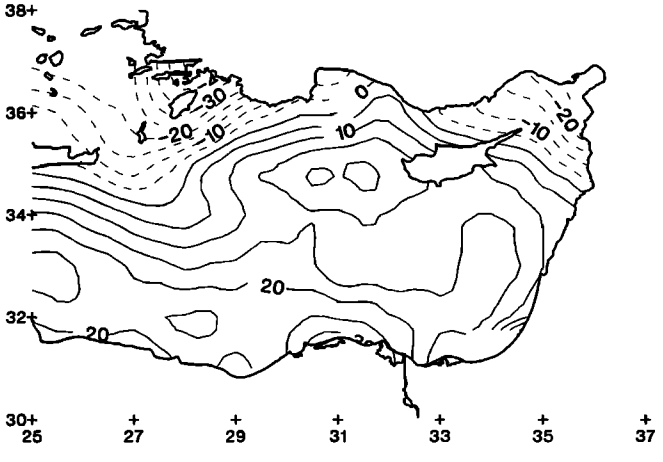


Fig. 3. Annual surface heat flux into the ocean (in watts per square meter) from the climatology of *May* [1983].

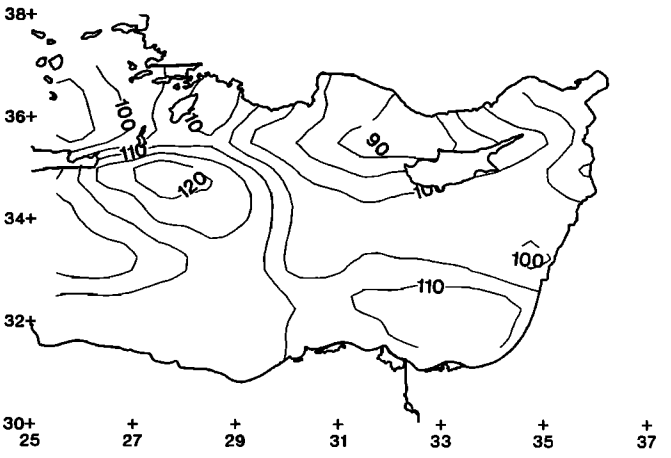


Fig. 4. Annual evaporation minus precipitation (in millimeters per month) using climatological observations from *May* [1983] and *Jaeger* [1976].

The surface layer of LSW is formed during summer by the intensive heating and evaporation. Below the summer mixed layer, the model reproduces the subsurface salinity minimum within the seasonal thermocline, which is subsequently weakened and masked by the deepening mixed layer during winter. The model forms this feature through the imposed steady advection of fresh water that compensates for the annual surface water loss. In contrast, this observed summer signal has often been attributed to the summer maximum in the inflow of the relatively fresh NAW through the Straits of Sicily. However, our results indicate that the seasonal cycle of the subsurface salinity minimum can be reproduced even with a steady advection of fresh water.

In the Rhodes gyre, the March mixed layer deepens to 250 m and acquires LIW characteristics with a temperature of 15.4°C and a salinity of 39.0 (Figure 5*a*). The water mass is only formed in winter, as the summer mixed-layer temperatures are much higher than the LIW values.

At the southern location, the LIW water mass is centered around a depth of 200 m, which is below the winter mixed layer and within the main thermocline (Figure 5*b*). This suggests that the LIW is not locally formed in the mixed layer here, which is always shallower and more buoyant but may instead be advected from a different source region, such as the Rhodes gyre.

### 4.4. *Mixed-Layer Model Integrations Over the Levantine Basin*

As the mixed-layer model produces reasonable seasonal profiles in two different locations, we now integrate the model separately for each 0.5° × 0.5° grid point covering the whole Levantine basin. The model is initialized with autumn (November) profiles taken from the *Naval Oceanographic Office* [1989] and forced by the corresponding surface heat, water, and momentum fluxes calculated from *May* [1982, 1983] and *Jaeger* [1976]. The model integration is performed

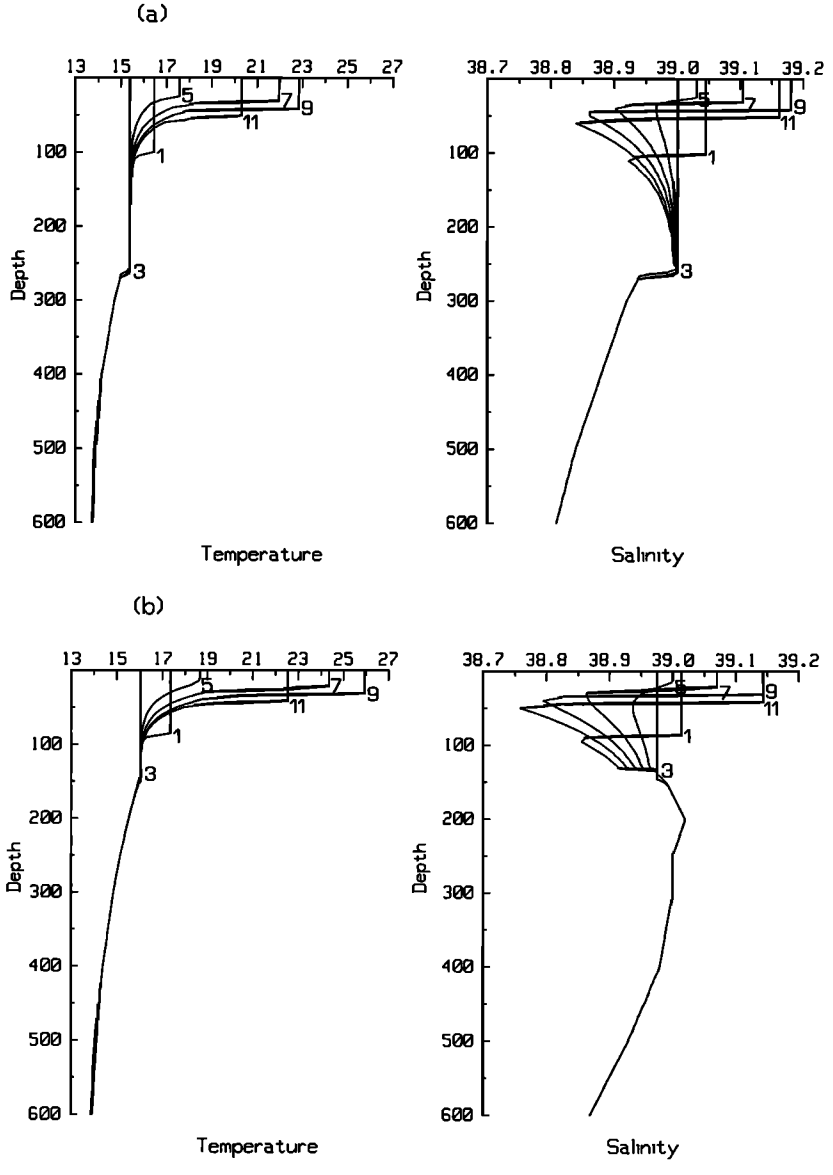


Fig. 5. Mixed-layer model profiles of temperature and salinity bimonthly over 1 year for (*a*) inside the Rhodes gyre (35°N, 28°E), and (*b*) a southern site at 33.5°N, 28.5°E.

separately at each grid point, producing a set of individual profiles, without any water mass being directly advected between neighboring grid points. In this section, we first force the model with surface fluxes and no parameterized advection and then second include the parameterized horizontal advection to obtain a closed annual cycle.

4.4.1. *Forcing by surface fluxes.* The model forced only by the surface fluxes produces LIW in the mixed layer (with density values between 28.85 and 29.10) during winter over the Northwest Levantine, which includes the cold, cyclonic Rhodes gyre; see Figure 6*a* for the March mixed-layer density after 4 months integration with LIW values indicated by dashed lines. Elsewhere, the mixed layer densities are too low to directly form LIW, unless one invokes extensive diabatic mixing in the thermocline.

The mixed-layer model though does not have a closed cycle, since the annual buoyancy loss over most of the basin leads to the mixed layer becoming denser every year. The drift in the model leads to the formation region of LIW artificially moving south and east in the March of the second year of integration (Figure 6*b*).

4.4.2. *Forcing by surface fluxes and parameterized advection.* The mixed-layer model integration is now forced by a parameterized horizontal advection (section 3.3), as well as by the surface fluxes. This is the model integration that we have most confidence in and will be referred to as the reference case. At each separate grid point, the diagnosed advection supplies enough cold and fresh water within the seasonal thermocline to offset the annual surface heat and water loss. While the diagnosed advection does lead to some plausible results, such as the subsurface salinity minimum signal (section 4.3), it is not dynamically calculated and does not communicate water-mass changes between grid points; it should be regarded primarily as a device to obtain a closed mixed-layer cycle.

The mixed-layer model now forms LIW repeatedly every March over the same region of the Northwest Levantine basin; see Figure 7*a* for the March density field after 16

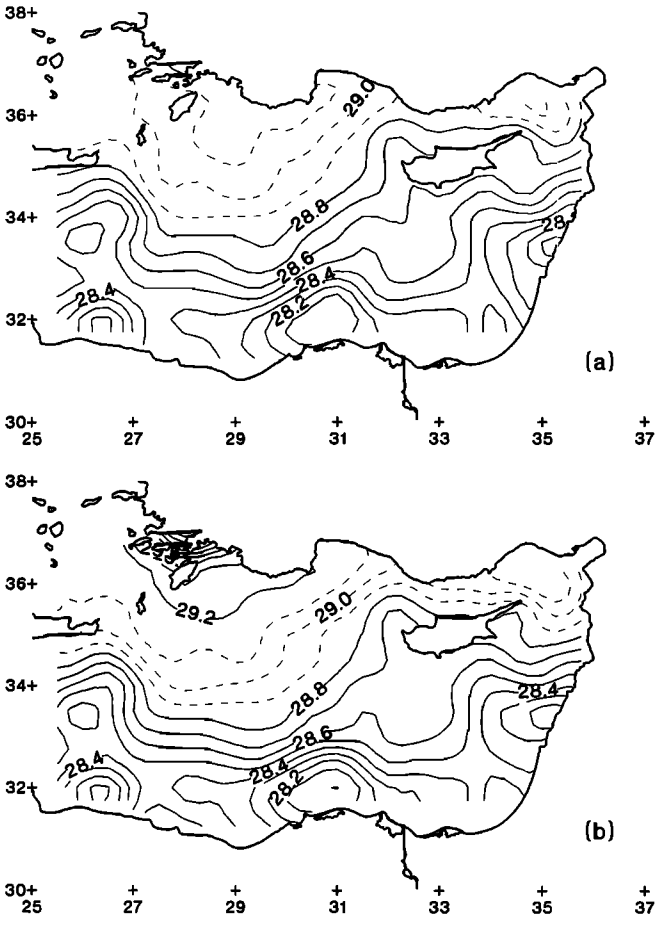


Fig. 6. Mixed-layer model density fields in March of (*a*) the first year and (*b*) the second year of integration, with forcing only from the surface fluxes.

months integration. The relatively dense water associated with LIW (values between 28.85 and 29.10) are associated with a March mixed layer reaching depths of more than 200 m, whereas it is generally shallower than this over the rest of the basin (Figure 7*b*).

The mixed-layer density field is principally controlled by the temperature variation (Figure 8*a*). The region of preferred LIW formation with temperatures between 15.0° and 16.0°C again lie over the Northwest Levantine. In contrast, the mixed layer has the appropriate salinities for LIW, from 38.95 to 39.05 psu, over much of the Levantine basin (Figure 8*b*). Thus temperature or density is useful in identifying where LIW is formed in the Levantine basin, while the salinity becomes important in identifying the water mass once it is subducted into the main thermocline and spreads over the Mediterranean.

The source region of LIW appears to be related to the outcropping of the isopycnals over the Rhodes gyre associated with the cyclonic circulation there, together with the spatial distribution of the annual heat and water fluxes over the Levantine basin. The sensitivity of the model to these processes is investigated in section 5.

The mixed-layer temperature differences between the model results and the climatological data are shown in Figure 9 for February and August. In February, the model produces a mixed layer that is marginally too cold by less than 0.5°C over the northern part of the basin, whereas it is too warm by typically 1°C toward the south in comparison with the climatology. In the summer, these differences become larger; the model is too warm by typically 1°C in the north and by more than 3°C in the south. Thus the model appears to simulate the winter reasonably well and is useful in studying the formation of water masses then but is less successful in simulating the summer climatology.

### 4.5. *Formation Rate of Levantine Intermediate Water*

In the reference integration, LIW begins to form within the mixed layer starting in mid-January, with the volume of LIW growing with the surface buoyancy loss, until a maximum volume is reached close to the spring equinox; the time history of this water mass within the mixed layer over the Levantine basin is shown in Figure 10. The layer of LIW water within the winter mixed layer is then subsequently capped by the spring warming and shallowing of the mixed layer. We believe that the layer of LIW is subducted into the thermocline, then spreads over the entire basin, ultimately with it passing through the Straits of Sicily.

The formation rate of LIW is estimated from the maximum volume of LIW found within the mixed layer over the Levantine basin divided by 1 year. This formation rate is estimated to be 1.0 Sv for climatological forcing; the sensitivity to interannual variability is examined in section 5.2.

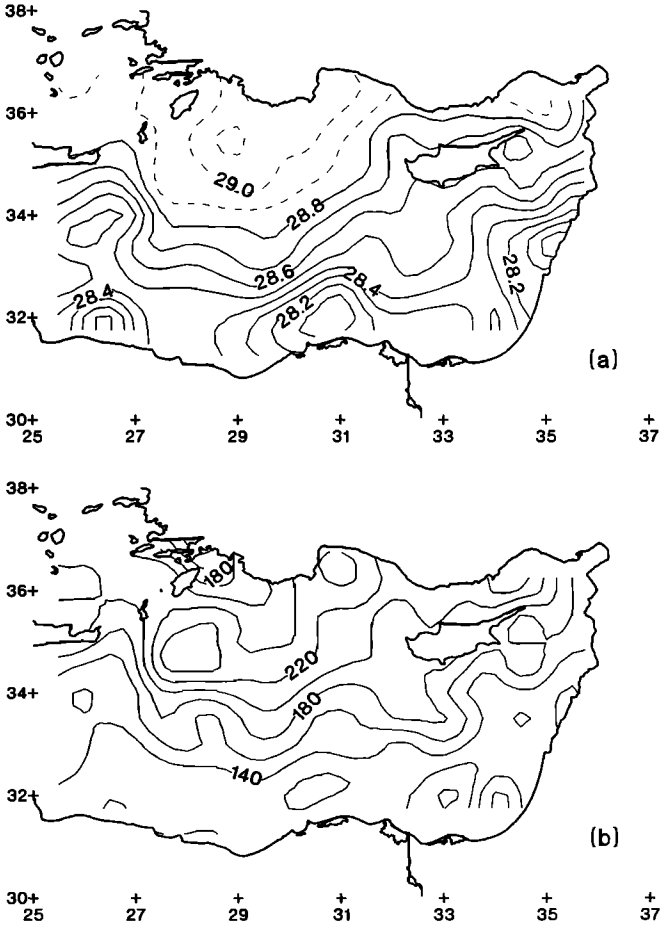


Fig. 7. Mixed-layer model (*a*) density and (*b*) thickness fields in March of the second year of integration with the model forced by surface fluxes and parameterized horizontal advection.

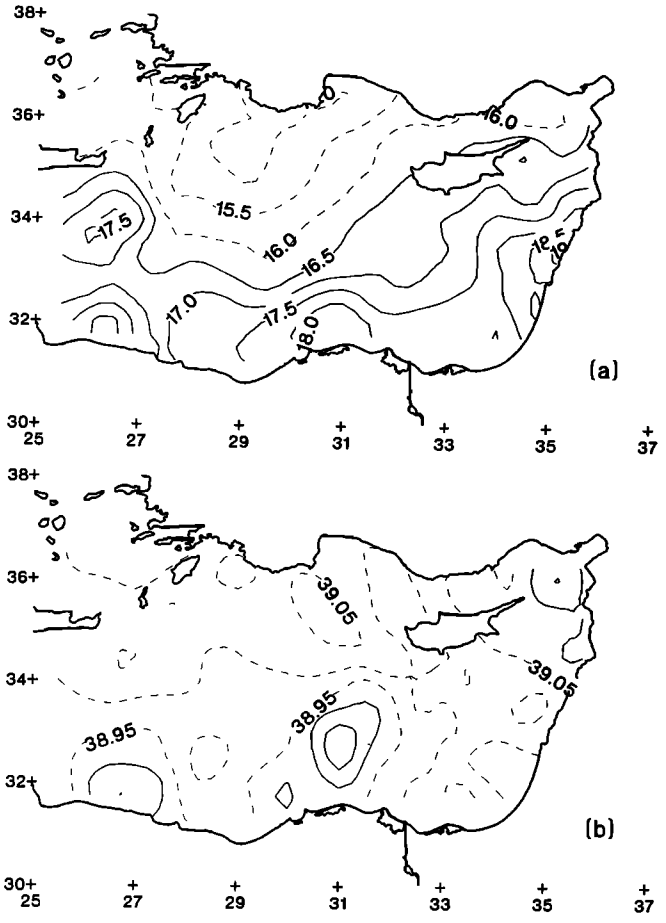


Fig. 8. Mixed-layer model (*a*) temperature and (*b*) salinity fields in March of the second year of integration with the model forced by surface fluxes and parameterized horizontal advection.

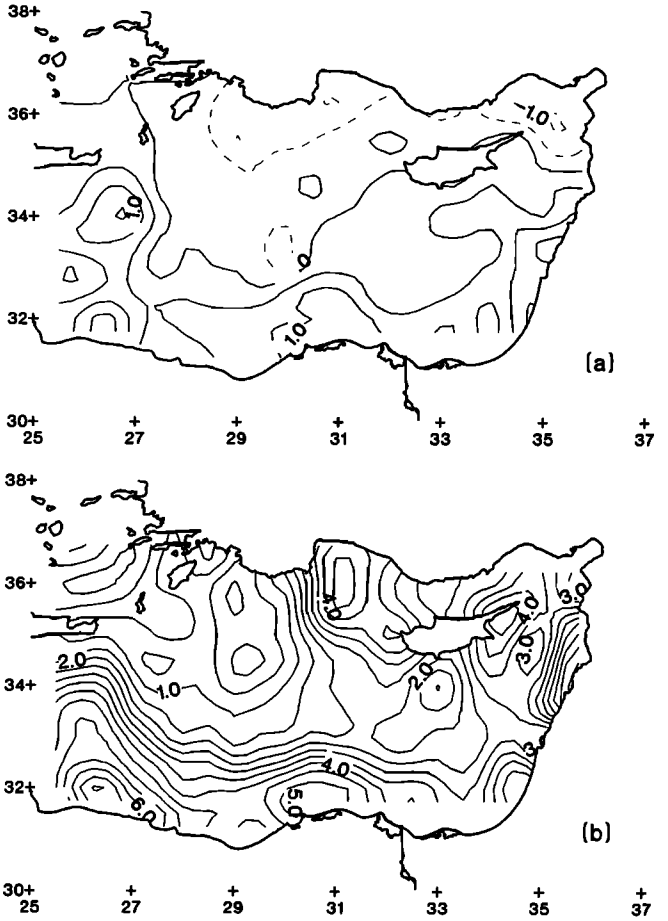


Fig. 9. Differences between the model and climatology temperature fields in (*a*) February and (*b*) August. The model results are in the second year of integration, with forcing by surface fluxes and horizontal advection, and the climatology from *Davis et al.* [1986].

This might overestimate the volume of LIW water that actually enters the main thermocline, as some of this subducted fluid may be reentrained into the mixed layer in the following winter [*Marshall et al.*, 1993]. However, our climatological estimate compares favorably with other independent estimates. *Tziperman and Speer* [1993] diagnose from the surface buoyancy forcing that the formation rate is 1.5 Sv for water masses with $\sigma_t > 28.80$ (note that we define LIW for a smaller $\sigma_t$ range from 28.85 to 29.10). In addition, *Ovchinnikov* [1983] estimates that the annual outflow of LIW through the Straits of Sicily is 1.23 Sv.

## 5. Sensitivity Studies of LIW Formation

### 5.1. *Control of the Formation Site*

We now investigate how the formation of LIW over the Rhodes gyre is controlled by either the patterns of the surface forcing or the preconditioning of the hydrography.

5.1.1. *Spatially uniform hydrography.* In this experiment, the model is initialized everywhere with the same autumn profile from a spatial average over the Levantine Basin. The model is integrated for 16 months with the climatological surface fluxes. The resulting mixed-layer density field in March is spatially uniform and does not show any pattern similar to that of the reference integration (Figure 11*a*); this is partly due to the horizontal advection compensating for the surface fluxes.

If this idealized experiment is repeated without incorporating the horizontal advection, then LIW is still not formed anywhere in the basin with the densest water produced in the northwest and northeast corners of the basin (Figure 11*b*). The pattern of the March mixed-layer density field now appears to be controlled by the pattern of the annual surface

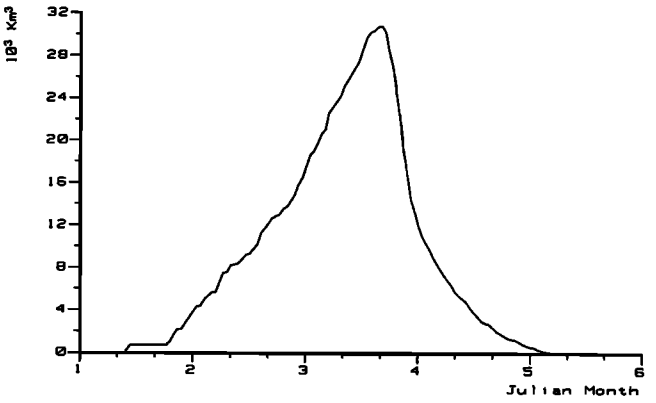


Fig. 10. Time history of the modeled volume of LIW ($10^3$ km$^3$) within the mixed layer over the Levantine basin.

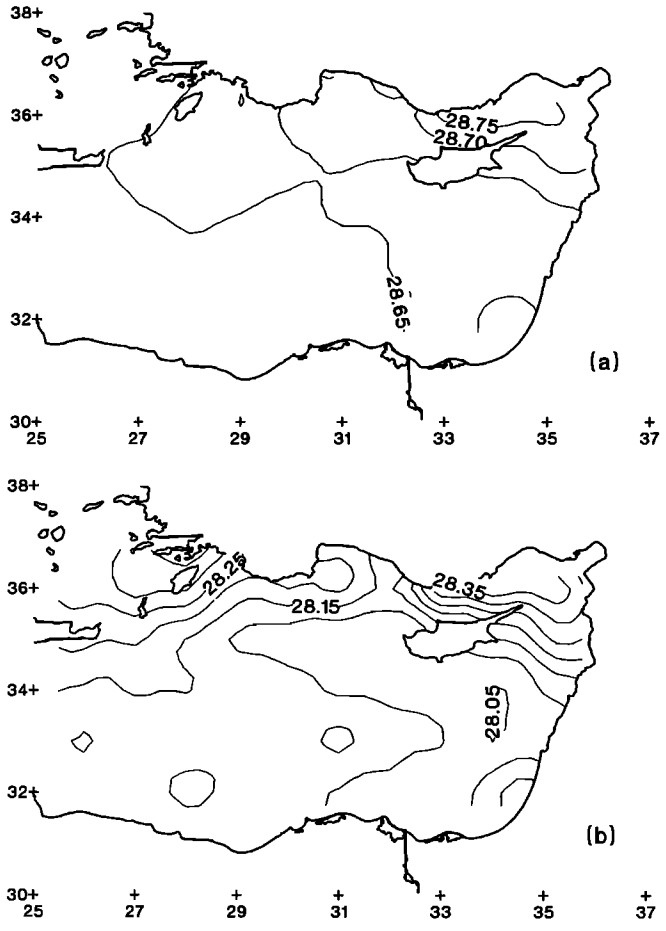


Fig. 11. Mixed-layer model density field in March after being initialized with spatially uniform hydrography in November and integrated for 16 months with (*a*) forced by surface fluxes and parameterized horizontal advection and (*b*) forced only by surface fluxes.

buoyancy forcing, itself mainly determined by the spatial structure of the surface heat loss (Figure 3). Therefore, while the surface fluxes enhance the formation of cool, dense fluid in the northern corners of the basin, they do not appear to be

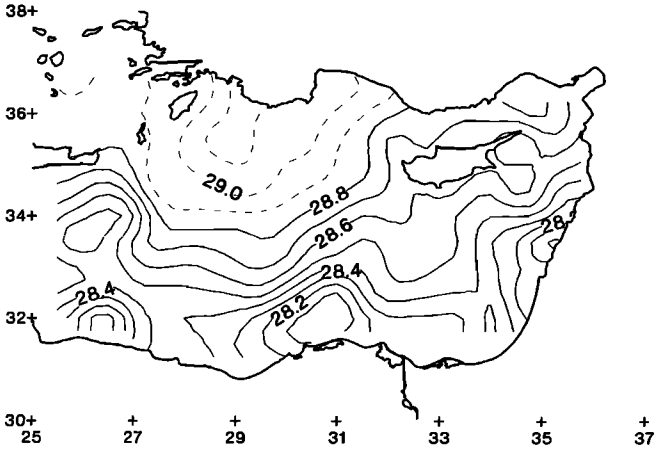


Fig. 12. Mixed-layer model density field in March after forcing by spatially uniform fluxes and parameterized advection, with the model initialized with spatially varying hydrography in November, and integrated for 16 months.

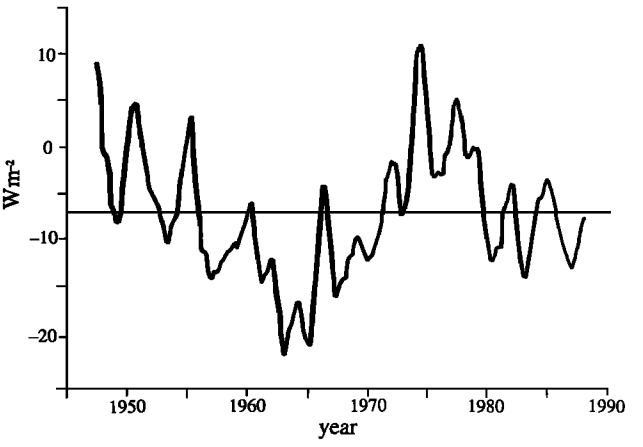


Fig. 13. Time history of the observed annual surface heat flux (in watts per square meter) out of the Mediterranean into the atmosphere (redrawn from *Garrett et al.* [1993]); the climatological mean is $-7$ W/m$^2$.

crucial in determining the preferred formation site over the Rhodes gyre.

5.1.2. *Spatially uniform surface fluxes.* In this case, the model is integrated with temporally varying, but spatially uniform surface fluxes. They have the mean values for the basin of an annual heat input of 8 W/m$^2$, a water deficit of 1.2 m/yr, and a wind speed of 4.9 m/s. The model is initialized here with the real spatially varying hydrography for autumn and integrated again for 16 months.

Despite using the spatially uniform fluxes, the model integration again forms LIW over the Rhodes gyre with the March mixed-layer density field (Figure 12) appearing similar to that of the reference integration (Figure 7). This suggests that the preconditioning of the hydrograph controls the preferred formation of LIW over the Rhodes gyre, rather than the pattern of the climatological fluxes.

### 5.2. *Interannual Variability in the Surface Fluxes*

We now investigate how sensitive the LIW formation might be to plausible variations in the magnitude of the annual surface heat flux.

The model is integrated for the reference case with climatological fluxes for 16 months (November to March) and then for a further year with extra surface heat fluxes, which are applied in addition to the background climatological forcing. At each grid point the parameterized horizontal advection terms are maintained at their initial climatological values; this probably gives an upper bound to the sensitivity of the mixed-layer, since the circulation is not allowed to change over 1 year and to compensate for the surface forcing.

In each experiment the additional heat fluxes are applied uniformly over the basin in amounts ranging from $-20$ to 20 W/m$^2$ in 5 W/m$^2$ increments; the results are found to be insensitive to whether this additional annual flux is spread over the cooling half of the year or the whole year. In comparison, year to year variations of the annual surface heat flux of the order of $\pm 5$ W/m$^2$ or even 10 W/m$^2$ seem to be quite frequent in the Mediterranean, as shown from Figure 13 [from *Garrett et al.*, 1993].

In the heating scenarios, the LIW formation zone reduces toward the Rhodes gyre, leading to smaller production rates.

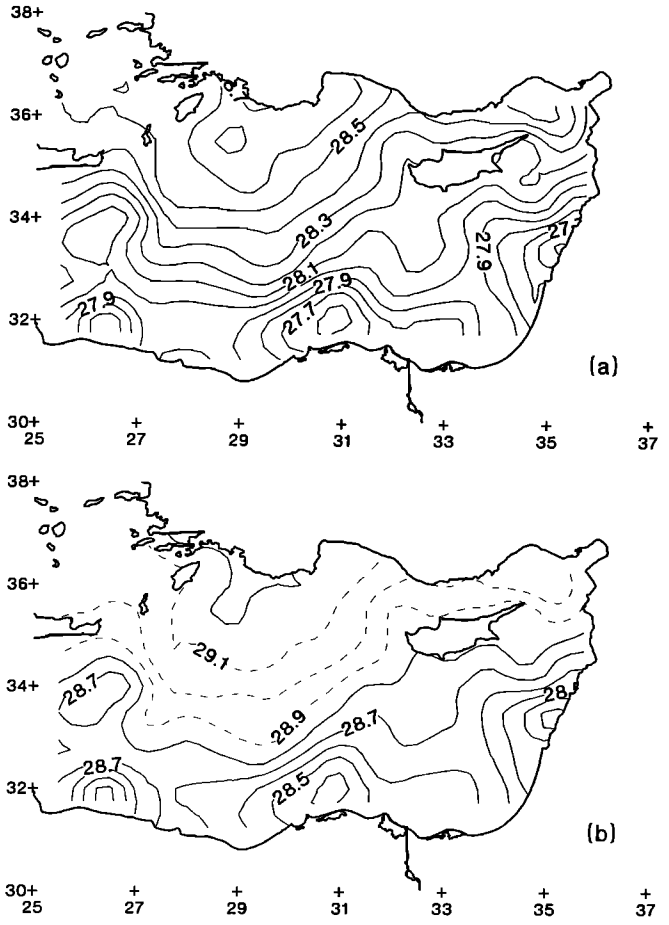


Fig. 14. Mixed-layer model density fields in March after 1 year integration with (*a*) an additional surface heat flux of 20 W/m$^2$ and (*b*) an additional surface heat flux of −20 W/m$^2$.

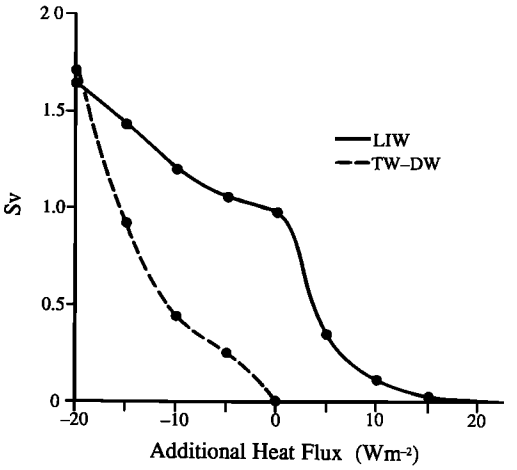


Fig. 15. Interannual sensitivity of the mixed-layer model formation (in sverdrups) rates of LIW and transition-deep water (TW-DW) versus additional annual surface heat fluxes into the ocean (in watts per square meter).

LIW production eventually ceases in the limiting case of the extra heating reaching +20 W/m$^2$ (Figure 14*a*).

In the cooling scenarios, the LIW production area moves farther to the east and south, while in the center of the Rhodes gyre, waters denser than LIW appear. In the limiting case of an extra cooling of −20 W/m$^2$ (Figure 14*b*), the March mixed layer deepens to over 1.5 km in the Rhodes gyre with the entrainment leading to low temperature of 14°C salinity of 38.94 psu, and a high density of 29.20. Therefore these deep chimneys contribute either to the Transition Waters, which lie below the LIW layer and above the Deep Waters layer, or even to the EMED Deep Waters.

The model results reveal that the production rates of LIW, and even Transition or Deep Waters (named here TW-DW), are sensitive to interannual variations in the surface heat fluxes (Figure 15).

The model predictions for severe winter conditions are indeed consistent with recent observations in the Levantine basin [*Sur et al.*, 1992] showing a deep chimney centered in the Rhodes gyre with TW-DW characteristics. Furthermore, the interannual variability experiments might explain claims of LIW production in areas such as the Southern Levantine under severe winter conditions [*Moros*, 1972], as well as the relative spread of the LIW characteristics found in literature (see Table 1).

## 6. Conclusions

The climatological study suggests that the Levantine Intermediate Water is only formed in the mixed layer at the end of winter over the northwestern part of the Levantine basin. The preferred production site appears to be controlled by the favorable preconditioning of the cold, cyclonic Rhodes gyre and, only to a lesser extent, by the pattern in the annual surface buoyancy input.

The annual LIW formation rate for climatological surface fluxes is found to be 1.0 Sv. This climatological estimate is sensitive though to variations in the magnitude of the annual-mean surface heat flux. An additional heat flux of 10 W/m$^2$ leads to the production rate of LIW reducing to 0.1 Sv, while an additional cooling of −10 W/m$^2$ enhances the production rate to 1.2 Sv. In the case of extreme cooling of an additional −20 W/m$^2$, the formation region of LIW moves eastward and southward, while at the same time, waters denser than LIW are produced at the center of the Rhodes gyre, which may contribute to the Transition or even Deep Waters of the Eastern Mediterranean.

Therefore, the mixed-layer model experiments suggest that the Rhodes gyre identifies where the most dense water is formed in the Levantine basin, whereas the magnitude of the surface fluxes determine whether this dense water falls within the water mass definition of LIW.

*Acknowledgments.* This work has been conducted in the framework of CEC/DGXII/MAST-039 Mediterranean Eddy Resolving Model And InterDisciplinary Studies (MERMAIDS) research project. We are grateful to John Marshall for helping to stimulate this study and to Paola Malanotte-Rizzoli and Chris Garrett for helpful advice and discussions; thanks also to Kostas Nittis for assistance with the figures. R.G.W. was supported under the NOAA Program in Climate and Global Change. Visits by E.T. to Imperial College and MIT have been financially supported by MAST.

## References

Brenner, S., Z. Rozentraub, J. Bishop, and M. Krom, The mixed-layer/thermocline cycle of a persistent warm core eddy in the Eastern Mediterranean, *Dyn. Atmos. Oceans*, 15, 457–476, 1991.

Budyko, M. I., *Climate and Life*, 508 pp., Academic, San Diego, Calif., 1974.

Davis, M. D., K. A. Countryman, and M. J. Carron, Tailored acoustic products utilizing the NAVOCEANO GDEM, paper presented at the Naval Symposium on Underwater Acoustics, San Diego, Calif., April 1–3, 1986.

Friedrich, H., Simulation of the thermal stratification at the FLEX central station with a one-dimensional integral model, in *North Sea Dynamics*, pp. 396–411, Springer-Verlag, New York, 1983.

Garrett, C., R. Outerbridge, and K. Thompson, Interannual variability in the Mediterranean heat and water fluxes, *J. Clim.*, *6*, 900–910, 1993.

Hecht, A., The hydrology and the water masses of the Eastern Mediterranean Sea, in *Proceedings of UNESCO/IOC First POEM Workshop, Erdemli-Icel, Turkey, 1986*, Part 2, *POEM Sci. Rep. 1*, edited by A. R. Robinson and P. Malanotte-Rizzoli, p. 51, Harvard University, Cambridge, Mass., 1986.

Hecht, A., N. Pinardi, and A. Robinson, Currents, water masses, eddies and jets in the Mediterranean Levantine basin, *J. Phys. Oceanogr.*, *18*, 1320–1353, 1988.

Hopkins, T. S., Physical processes in the Mediterranean basins, in *Estuarine Transport Processes*, edited by B. Kjerfve, pp. 269–309, University of South Carolina Press, Columbia, 1978.

Horch, A., W. Barkmann, and J. D. Woods, Die Erwarmung des Ozeans hervorgerufen durch solare Strahlungsenergie, *Ber. Inst. Meereskd. Univ. Kiel*, 120, 190 pp., 1983.

Jaeger, L., Monatskarten des Niedersschlags fur die gange Erde, *Ber. Dtsch. Wetterdenstes*, *18*(139), 38 pp., 1976.

Kato, H., and O. M. Phillips, On the penetration of a turbulent layer into a stratified layer, *J. Fluid Mech.*, *37*, 643–655, 1969.

Katz, E. J., The Levantine Intermediate Water between the Strait of Sicily and the Strait of Gibraltar, *Deep Sea Res.*, *19*, 111–520, 1972.

Kraus, E. B., and J. S. Turner, A one-dimensional model of the seasonal thermocline, II, The general theory and its consequences, *Tellus*, *19*, 98–105, 1967.

Lacombe, H., and P. Tchernia, Quelques traits generaux de l'hydrologie Mediterranee, *Cah. Oceanogr.*, *12*, 527–547, 1960.

Lacombe, H., and P. Tchernia, Caracters hydrologiques et circulation des eaux en Mediterranee, in *The Mediterranean Sea: A Natural Sedimentation Laboratory*, edited by D. J. Stanley, pp. 25–36, Dowden, Hutchinson and Ross, Stroudsburg, Pa., 1972.

Large, W. G., and S. Pond, Open ocean momentum flux measurements in moderate to strong winds, *J. Phys. Oceanogr.*, *11*, 324–336, 1981.

List, R. J., *Smithsonian Meteorological Tables*, Smithsonian Institution, Washington, D. C., 1966.

Malanotte-Rizzoli, P., and A. Bergamasco, The wind and thermally driven calculation of the eastern Mediterranean Sea, II, The Baroclinic case, *Dyn. Atmos. Oceans*, *15*, 355–419, 1991.

Malanotte-Rizzoli, P., and A. Hecht, Large-scale properties of the Eastern Mediterranean: A review, *Oceanol. Acta*, *11*(4), 323–335, 1988.

Marshall, J. C., A. J. G. Nurser, and R. G. Williams, Inferring the subduction rate and period over the North Atlantic, *J. Phys. Oceanogr.*, *23*(7), 1315–1329, 1993.

May, P., Climatological flux estimates in the Mediterranean Sea, 1, Wind and wind stresses, *NORDA Rep.*, *54*, 56 pp., Nav. Ocean Res. and Dev. Activ., NSTL Station, Miss., 1982.

May, P., Climatological flux estimates in the Mediterranean Sea, 2, Air sea fluxes, *NORDA Rep.*, *58*, 65 pp., Nav. Ocean Res. and Dev. Activ., NSTL Station, Miss., 1983.

Morcos, S. A., Sources of Mediterranean Intermediate Water in the Levantine Sea, in *Studies in Physical Oceanography: A Tribute to G. Wust on his 80th Birthday*, vol. 2, edited by A. L. Gordon, pp. 185–206, Gordon and Breach, New York, 1972.

Morel, A., Caracteres hydrologiques des eaux echangees entre le bassin Oriental et le bassin Occindetal de la Mediterranee, *Cah. Oceanogr.*, *23*, 329–342, 1971.

Mosetti, F., E. Accerboni, and A. Lavenia, Recherches oceanographiques en Mediterranee orientale (Aout 1967), *Rapports et Proces-Verbaux des Reunions. Commission Internationale pour l'Exploration Scientifique de la Mediterranee*, *20*, 623–625, 1972.

Naval Oceanographic Office, GDEM, Data base description for master generalized digital environmental model, 15 pp., Environ. Syst. Div., Stennis Space Center, Miss., 1989.

Nielsen, J. N., Hydrography of the Mediterranean and adjacent waters, in *Report of the Danish Oceanographic Expedition 1908–1910 to the Mediterranean and Adjacent Waters*, vol. 1, pp. 72–191, Copenhagen, 1912.

Niiler, P. P., and E. B. Kraus, One-dimensional models of the upper ocean, in *Modelling and Predictions of the Upper Layers of the Ocean*, edited by E. B. Kraus, 325 pp., Pergamon, Elsmford, N. J., 1977.

Oren, O. H., The Atlantic water in the Levant Basin and on the shores of Israel, *Cah. Oceanogr.*, *23*, 291–297, 1971.

Ovchinnikov, I. M., The sixth Mediterranean expedition on the Research Vessel *Akademik S. Vavilov*, *Oceanology*, *4*, 143–148, 1965.

Ovchinnikov, I. M., Circulation in the surface and intermediate layers of the Mediterranean, *Oceanology*, *6*, 48–57, 1966.

Ovchinnikov, I. M., On the water balance of the Mediterranean Sea, *Oceanology*, *14*, 198–202, 1974.

Ovchinnikov, I. M., The renewal of the principal water masses of the Mediterranean, *Oceanology*, *23*, 719–721, 1983.

Ovchinnikov, I. M., The formation of Intermediate Water in the Mediterranean, *Oceanology*, *24*, 168–173, 1984.

Ovchinnikov, I. M., and A. Plakhin, Formation of the intermediate waters of the Mediterranean Sea in the Rhodes cyclonic gyre, *Oceanology*, *24*, 317–319, 1984.

Ozsoy, E., A. Hecht, and U. Unluata, Circulation and hydrography of the Levantine Basin: Results of POEM coordinated experiments 1985–1986, *Prog. Oceanogr.*, *22*, 125–170, 1989.

Ozturgut, E., The source and spreading of the Levantine Intermediate Water in the eastern Mediterranean, *Memo. SM-92*, Saclant ASW Res. Cent., 45 pp., La Spezia, Italy, 1976.

Plakhin, A., and V. G. Smirnov, On the determination of initial T, S—Indices of the Mediterranean Sea waters, *Oceanology*, *24*, 174–177, 1984.

POEM Group, General circulation of the Eastern Mediterranean, *Earth Sci. Rev.*, *32*, 285–308, 1992.

Robinson, A. R., M. Golnaraghi, W. G. Leslie, A. Artegiani, A. Hecht, E. Lassoni, A. Michelato, E. Sansone, A. Theocharis, and U. Unluata, The Eastern Mediterranean general circulation: Features, structure and variability, *Dyn. Atmos. Oceans*, *15*, 215–240, 1991.

Schlitzer, R., W. Roether, H. Oster, H-G. Junghans, M. Hausmann, H. Johanssen, and A. Michelato, Chlorofluoromethane and oxygen in the Eastern Mediterranean, *Deep Sea Res.*, *38*, 1531–1551, 1991.

Sur, H. I., E. Ozsoy, T. Oguz, and U. Unluata, Wide area formation of intermediate and deep water in the northern Levantine basin, *Rapp. Comm. Int. Mer Méditer.*, *33*, 235, 1992.

Thompson, R. O. R. Y., Climatological numerical models of the surface mixed layer at the ocean, *J. Phys. Oceanogr.*, *6*, 496–503, 1976.

Tziperman, E., and K. Speer, A study of water mass transformation in the Mediterranean Sea: Analysis of climatological data and a simple 3-box model, *Dyn. of Atmos. Oceans*, in press, 1993.

UNESCO, Physical oceanography of the Eastern Mediterranean: An overview and research plan, *UNESCO Rep. Mar. Sci.*, *30*, 36 pp., 1984.

Williams, R. G., The influence of air-sea interaction on ocean synoptic-scale eddies, Ph.D. thesis, Univ. of East Anglia, Norwich, England, 1987.

Williams, R. G., Modification of ocean eddies by air-sea interaction, *J. Geophys. Res.*, *93*, 15,523–15,533, 1988.

Woods, J. D., and W. Barkmann, The response of the upper ocean to solar heating, I, The mixed-layer, *Q. J. R. Meteorol. Soc.*, *112*, 1–27, 1986.

Wust, G., On the vertical circulation of the Eastern Mediterranean Sea, *J. Geophys. Res.*, *66*, 3261–3271, 1961.

Zore-Armanda, M., Water exchange between the Adriatic and the Eastern Mediterranean, *Deep Sea Res.*, *16*, 171–178, 1969.

A. Lascaratos and E. Tragou, Laboratory of Meteorology and Oceanography, Department of Applied Physics, University of Athens, 33 Ippocratous Str., 10680 Athens, Greece.

R. G. Williams, Center for Meteorology and Physical Oceanography, Department of Earth, Atmospheric and Planetary Sciences, Massachusetts Institute of Technology, Cambridge, MA 02139.

(Received June 30, 1992;
revised April 6, 1993;
accepted April 6, 1993.)